

112498



U.S. Department of Transportation

National Highway Traffic Safety Administration

Memorandum

Vehicle Research and Test Center

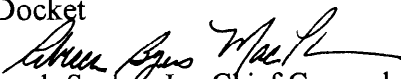
P.O. Box 37
East Liberty, Ohio 43319-0337
(937) 666-4511

Subject: Submission to Docket No. NHTSA-2000-6940 - 10
Report titled, "Impact Loading to the Chin of the Hybrid III Small Female Dummy Head and Neck System"

Date: SEP 27 2000

From: Daniel A. Rhule 
Pedestrian and Applied Biomechanics Division

Reply to Attn. of: NRD-21

To: NHTSA Docket

THRU: Frank Seales, Jr., Chief Counsel

SEP 27 2000
NHTSA

Attached is a technical report summarizing experimental testing of the Hybrid III small female head and neck system. In order to investigate the dynamic bending response of the Hybrid III small female neck to a head impact, a series of tests were conducted to simulate the impact of an air bag to the head of the dummy. A pendulum impactor was used to strike the chin of the dummy head, simulating impacts in both the horizontal (fore-aft) and vertical (superior-inferior) orientations. The study also investigates the role of the nodding block stiffness and neck cable to the overall bending response of the neck system.

Please include the attached document in the Docket No. NHTSA-2000-6940.

Attachment

#

**Impact Loading to the Chin
of the
Hybrid III Small Female Dummy
Head and Neck System**

**Dan Rhule
Vehicle Research and Test Center
Sept. 2000**

Background

In order to investigate the dynamic bending response of the Hybrid III small female neck to a head impact, a series of tests were conducted to simulate the impact of an air bag to the head of the dummy. A pendulum impactor was used to strike the chin of the dummy head, simulating impacts in both the horizontal (fore-aft) and vertical (superior-inferior) orientations.

X-Axis (Horizontal) Impacts

The head and neck assembly was rigidly mounted to a fixture as shown in Fig. 1. Seven impact tests were conducted in which the chin was struck parallel to the x-axis, approximately 2" below the occipital condyle. The orientation of the head was determined by placing the skull cap mounting surface as nearly vertical as possible. This may have been a potential source of error later in the testing when the neck cable was removed. Without the support of the neck cable, the neck tended to sag under the weight of the head, thus the orientation of the head relative to the neck may have varied slightly for tests in which no cable was used as compared to tests which utilized the neck cable. The impactor mass was 4.72 kg (10.4 lbs) and was dropped to achieve an impact velocity of 6.1 m/s (20 ft/s), except for test #1 which utilized a speed of 4.57 m/s (15 ft/s). The impactor had a 3" diameter impact surface with $\frac{1}{2}$ " radius.

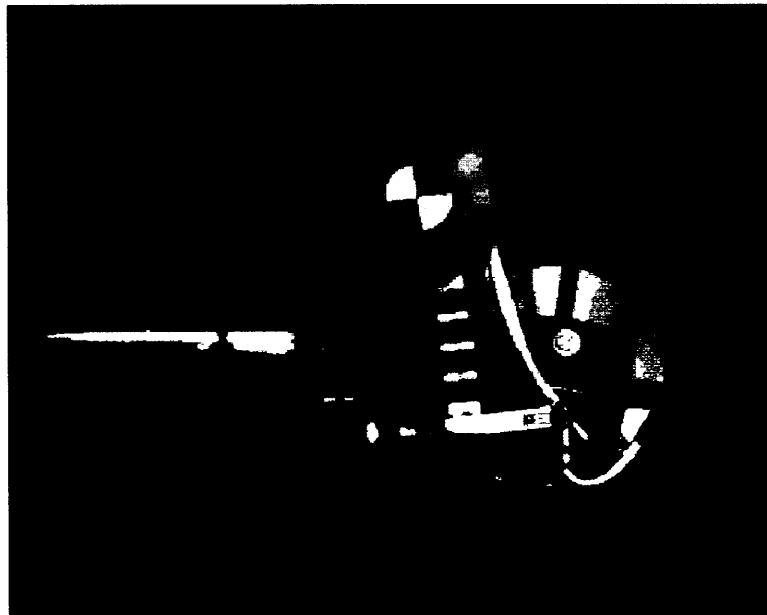


Fig. 1. X-Axis Chin Impact

The head and neck were instrumented with an upper and lower neck load cell, a tri-axial accelerometer array at the head CG and an extra z-axis accelerometer at the rear of the head. The angular displacement of the head was computed from the pair of z-axis accelerometers in the head. Analysis of the digital video verifies that the results of this computation is relatively accurate. For this study, a negative head angle represents a rotation in the flexion mode, while a positive angle represents a rotation in the extension mode.

The test matrix for x-axis impacts appears in Table 1.

Table 1. X-Axis Chin Impact Test Matrix

Test # 047800--	Impact Speed (ft/s)	Neck Cable Disposition	Nodding Block Disposition
01	15	assembled	standard
02	20	assembled	standard
05	20	assembled	75% nodding block
09	20	removed	standard
12	20	removed	50 % nodding block
14	20	removed	car seat foam
15	20	removed	Ensolute foam

Z-Axis (Vertical) Impacts

Four impact tests were conducted in which the chin was struck parallel to the z-axis, approximately 4" above the occipital condyle. The orientation of the head was determined by placing the skull cap mounting surface as nearly horizontal as possible. A typical test set-up is shown in Figure 2. A potential source of error may have developed later in the testing when the neck cable was removed. Without the support of the neck cable, the neck tended to sag under the weight of the head, thus the orientation of the head relative to the neck may have varied slightly for tests in which no cable was used as compared to tests which utilized the neck cable. The impactor mass was 4.72 kg (10.4 lbs) and was dropped to achieve an impact velocity of 6.1 m/s (20 ft/s). The impactor had a 3" diameter impact surface with 1/2" radius.

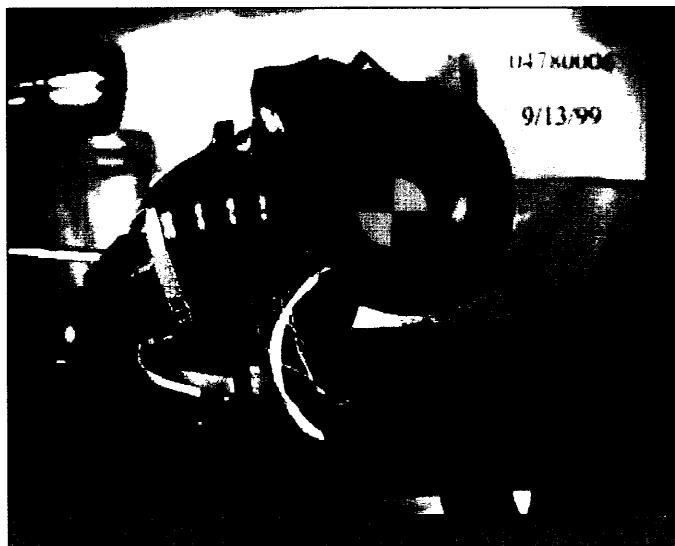


Fig. 2. Typical Test Setup for Z-axis Impacts

The test matrix for z-axis impacts appears in Table 2.

Table 2. Z-Axis Chin Impact Test Matrix

Test # 047800--	Impact Speed (ft/s)	Neck Cable Disposition	Nodding Block Disposition
03	20	assembled	standard
06	20	assembled	75% nodding block
10	20	removed	standard
11	20	removed	50 % nodding block

Nodding Blocks

The nodding blocks were modified several times in an attempt to study their influence to the total response. In tests 1, 2, 3, 9, and 10 the standard nodding blocks were used (see Fig. 3). In tests 5 and 6, 25% of the nodding block length was removed (see Fig. 4). In tests 11 and 12, 50% of the nodding block was removed (see Fig. 5). In tests 14 and 15, the nodding blocks were removed entirely and replaced with very soft materials - car seat foam in test 14; Ensolite in test 15. The purpose of these materials was primarily to prevent metal-to-metal contact between the neck load cell and the top surface of the neck assembly.

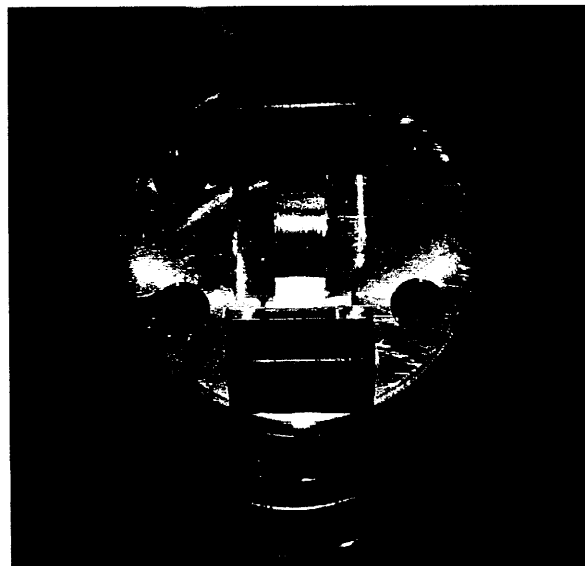


Fig. 3. Standard Nodding Blocks

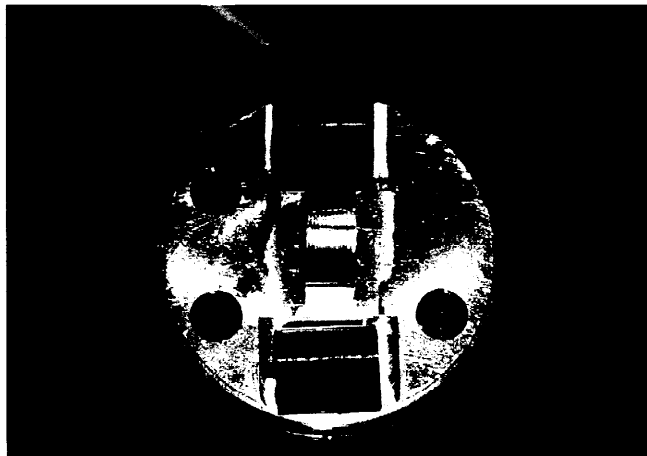


Fig. 4. 75% Nodding Blocks

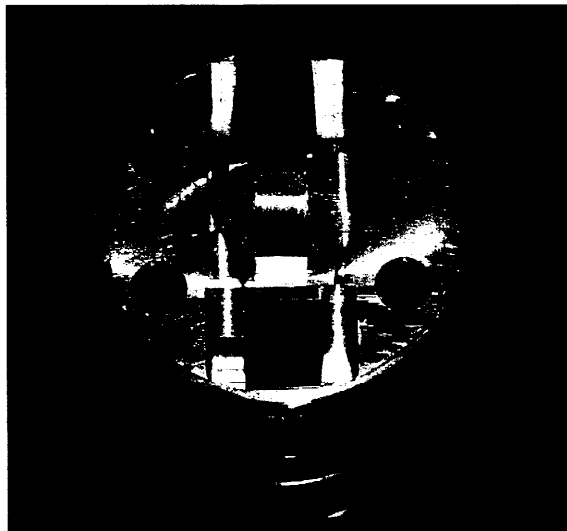


Fig. 5. 50% Nodding Blocks

Results of X-Axis Impacts

Head Angular Displacement

Upon impact, the head initially rotates in the flexion mode, followed by a reverse of rotation into extension. Table 3 below summarizes the peak flexion and extension angles and the timing of the events (assuming t_0 = time of impactor contact). Fig. X.1. provides the graphical time histories of the head angular displacements.

Table 3. X-axis Impact - Head Angular Displacement Peak Summary

	test #2		test #5		test #9		test #12		test #15	
	angle (deg)	time (ms)								
peak flexion	-6.68	7.1	-7.91	10.2	-8.12	11.2	-10.28	13.9	-11.23	11.6
peak extension	44.35	96	47.55	94.2	58.59	111.5	65.89	118.4	84.04	129.6

Moment About Occipital Condyle

The corrected moment about the occipital condyle was computed from the upper neck load cell. Figure X.2. provides the graphical time histories of the moment about the occipital condyle. The results indicate a large flexion peak moment early in the event, followed by a small extension moment later on. Table 4 below summarizes the peak flexion moments and the time of the peak flexion moment.

Table 4. X-axis Impact - Moment About Occipital Condyle Peak Summary

	test #2		test #5		test #9		test #12		test #15	
	moment (Nm)	time (ms)								
peak flexion	99.4	9.6	86.4	12.5	80.7	14.3	75.1	17.1	73.0	18.8

Axial Load

A graphical time history of the axial neck loads are provided in Fig. X.3. The results indicate an initial tension peak followed by a compression peak of magnitude nearly equal to that of the tension load. This entire cycle is complete before the head rotates into extension. Table 5 summarizes the peak flexion moments and the time of the peak flexion moment.

Table 5. X-axis Impact - Axial Load

	test #2		test #5		test #9		test #12		test #15	
	load (N)	time (ms)								
peak tension	1024.3	2.3	929.5	2.6	559.6	2.5	649.7	3.8	860.8	3.9
peak compression	-877.4	15.0	-652.3	15.7	-480.2	16.9	-435.1	17.9	-414.5	19.2

Moment versus Head Angular Displacement

Figures X.4. and X.5. are cross-plots of the moment about the occipital condyle versus the head angular displacement. Fig. X.4. presents the results over the entire event, while Fig. X.5. focuses on the initial onset of the moment until the time of peak flexion (note: the second chart contains the same data sets utilized in the first chart, but the data has been clipped after the initial rise to illustrate the differences in onset rates). From the second chart, the onset slope of the curve has been computed and these results are summarized in Table 6 below.

Table 6. X-axis Impact - Rate of Moment Onset

	test #2	test #5	test #9	test #12	test #15
flexion onset rate (Nm/deg)	13.6	10.0	9.1	6.1	4.8

Neck Shear Loads

Fig. X.6. contains the shear loading response recorded at the upper neck load cell. There is an initial inertial spike within the first three milliseconds followed by a secondary spike at approximately 10 to 15 milliseconds. Table 7 contains the values of the secondary peak.

Table 7. X-axis Impact - Neck Shear Loading Secondary Peak Summary

	test #2		test #5		test #9		test #12		test #15	
	load (N)	time (ms)								
peak shear	1427	9.3	1236	10.0	1092	10.4	1023	12.2	924	14.9

Results of Z-Axis Impacts

Head Angular Displacement

Table 8 below summarizes the peak extension angles and the timing of the events (assuming t_0 = time of impactor contact). Figure Z.1. provides the graphical time histories of the head angular displacements.

Table 8. Z-axis Impact - Head Angular Displacement Peak Summary

	test #3		test #6		test #10		test #11	
	angle (deg)	time (ms)	angle (deg)	time (ms)	angle (deg)	time (ms)	angle (deg)	time (ms)
peak extension	63.6	84.2	64.0	84.2	78.6	104.7	82.2	106.4

Moment About Occipital Condyle

The corrected moment about the occipital condyle was computed from the upper neck load cell. Figure Z.2. provides the graphical time histories of the moment about the occipital condyle. Table 9 below summarizes the peak extension moments and the times of the peak extension moments.

Table 9. Z-axis Impact - Moment About Occipital Condyle Peak Summary

	test #3		test #6		test #10		test #11	
	moment (Nm)	time (ms)						
peak extension	-53.6	12.3	-49.2	11.7	-40.9	14.0	-37.0	15.3

Neck Axial Loads

Table 10 below summarizes the peak axial loads and the time of the peaks. Fig. Z.3. shows the time history of the axial neck loads from the upper neck load cell. The results indicate an early tension peak load.

Table 10. Z-axis Impact - Axial Load

	test #3		test #6		test #10		test #11	
	load (N)	time (ms)						
peak tension	3223.9	2.3	3174.9	2.2	1771.0	1.8	1877.6	1.9

Moment versus Head Angular Displacement

Fig. Z.4. is a cross-plot of the moment about the occipital condyle versus the head angular displacement.

Neck Shear Loads

Fig. Z.5. provides a graphical time history of the neck shear loads. The results indicate a negative shear load peak (head forward relative to neck) occurring very early in the event. Table 11 below summarizes the peak shear loads and the times of the peaks.

Table 11. Z-axis Impact - Shear Load

	test #3		test #6		test #10		test #11	
	load (N)	time (ms)						
peak tension (N)	-1260.1	1.9	-1405.7	1.9	-1189.4	1.8	-1060.0	1.9

Discussion

X-axis Impacts

The X-axis impacts to the dummy chin exhibited high moment loads in excess of 100 Nm at small head flexion rotations of less than 10 degrees.

The various modifications to the nodding blocks and neck cable provided some reduction in the peak flexion moments and the moment onset rates. Table 12 shows the percent reduction in peak flexion moment for tests 5, 9, 12, and 15 as compared to the baseline (test 2). Table 13 shows the percent reduction in the moment onset rate.

Table 12. Reduction in Peak Flexion Moment as Compared to Baseline (Test #2)

	test #5	test #9	test #12	test #15
% reduction in peak flexion moment	13.1	18.9	24.4	26.6

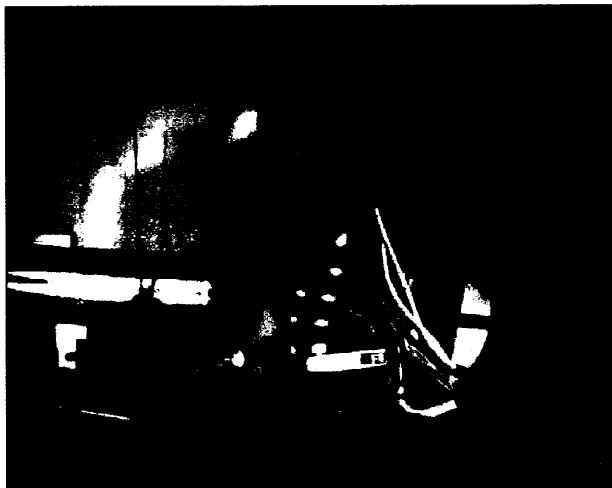
Table 13. Reduction in Moment Onset Rates as Compared to Baseline (Test #2)

	test #5	test #9	test #12	test #15
% reduction in moment onset	26.2	33.0	55.3	64.3

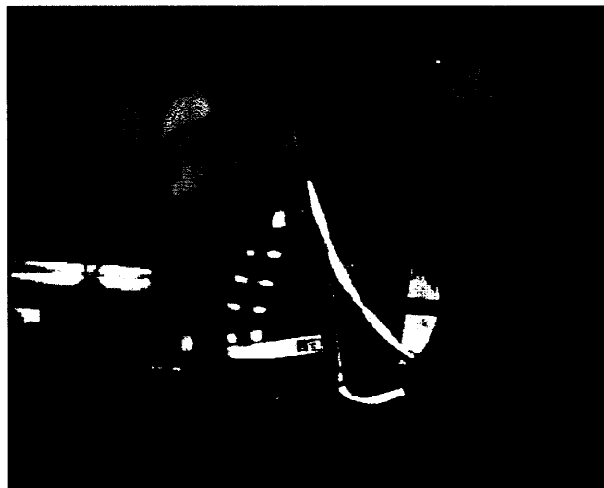
The head angular displacement results provide head rotation with respect to a fixed reference frame. This may be misleading when interpreting the results because it does not account for the motion of the neck relative to the head. Consider the four pictures in Fig.6. Each picture is from the instant of peak angular flexion for the four different tests (5, 9, 12, and 15). Notice that the attitude of the head changes only slightly between each test (with respect to the fixed reference frame), however, the angle formed by the bottom surface of the chin and the front surface of the neck changes more visibly each test. This phenomena will need to be considered further in the future. It may be more meaningful to plot the translation of multiple points on the head as a function of time to demonstrate not only the rotation, but also the translation of the head relative to the lower neck bracket.

Z-axis Impacts

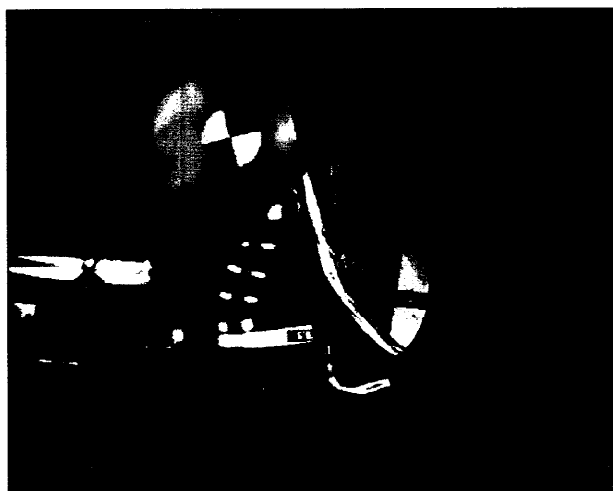
The removal of the neck cable had the largest effects on the resulting neck loads, while the changes to the nodding blocks had the least effect. Comparing the peak head rotation for tests 3 and 6 (neck cable assembled) with tests 10 and 11 (neck cable removed) the head rotated, on average, 20 degrees further when the cable was removed. The peak moment was 12.5 Nm less when the neck cable was removed and the peak axial load was 1375 N lower when the neck cable was removed.



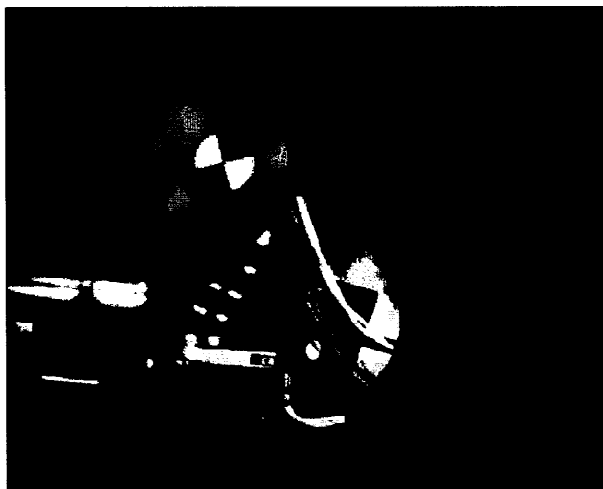
Test 5 Peak Flexion



Test 9 Peak Flexion



Test 12 Peak Flexion



Test 15 Peak Flexion

Fig. 6. Head Attitude at Time of Peak Flexion

**X-axis Impacts
Head Angle vs. time**

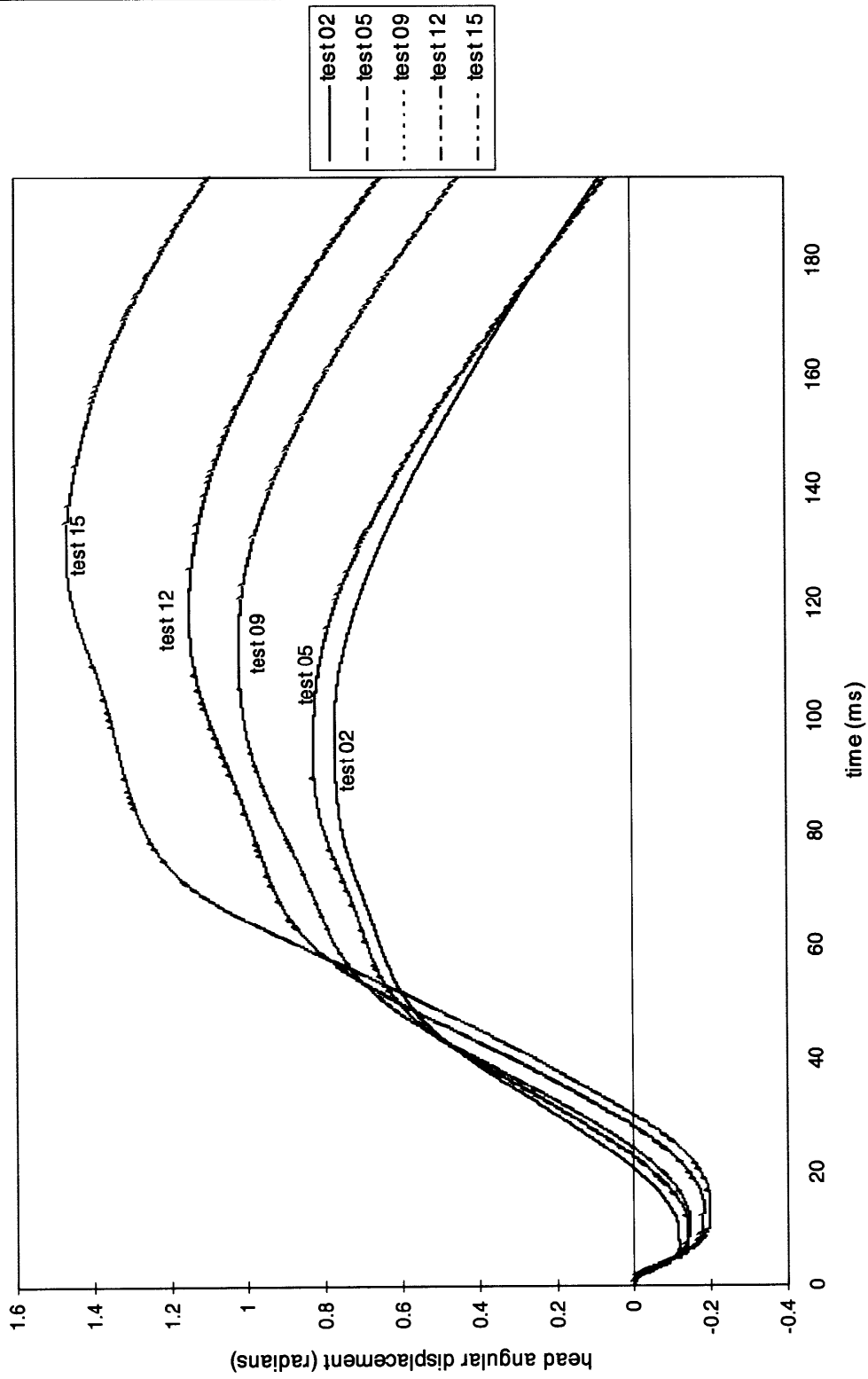


Fig. X.1. X-axis Impacts - Head Rotations

**X-Axis Impacts
Moment vs. Time**

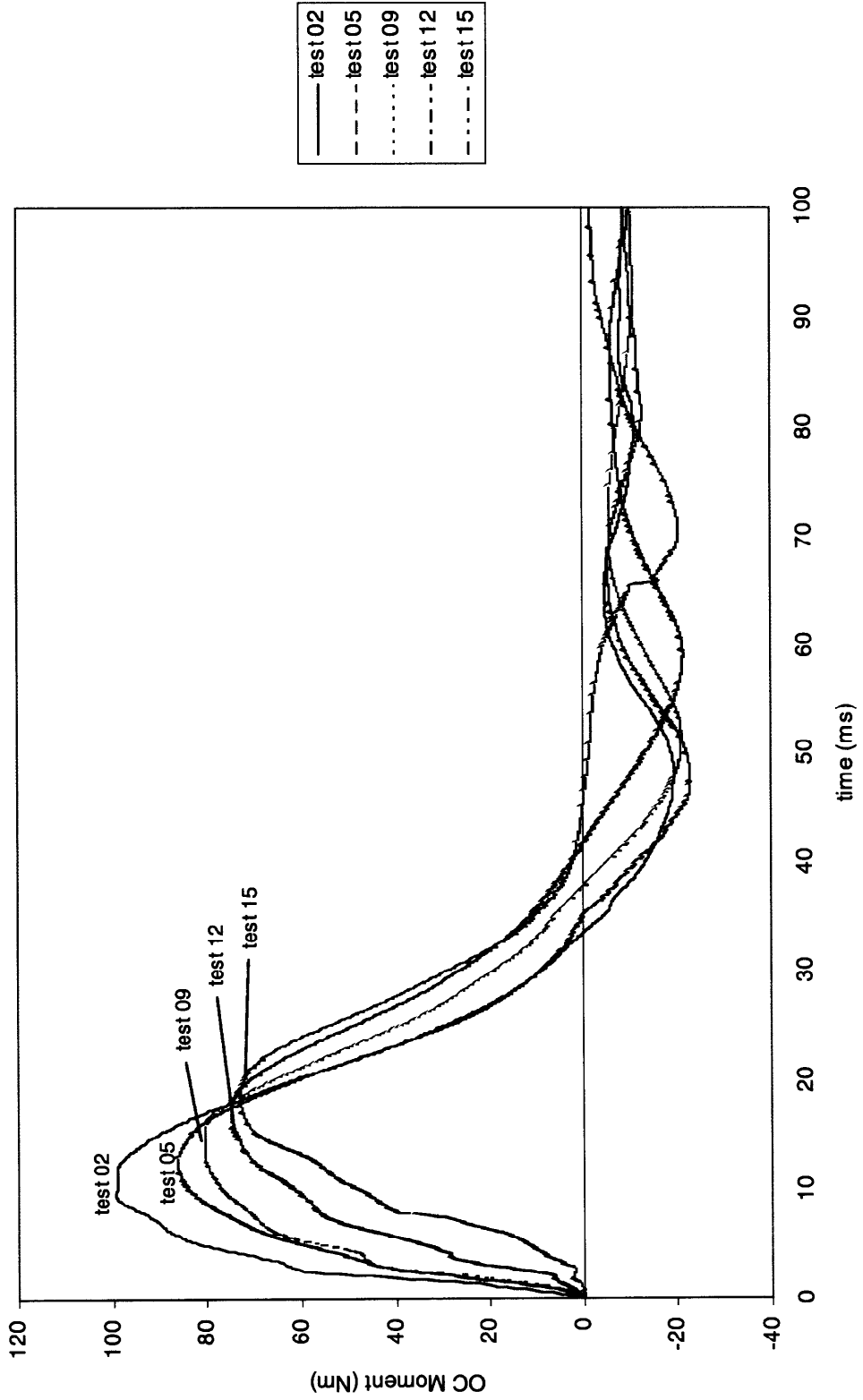


Fig. X.2. X-axis Impacts - Neck Moment About Occipital Condyle

**X-Axis Impacts
Axial Load vs. time**

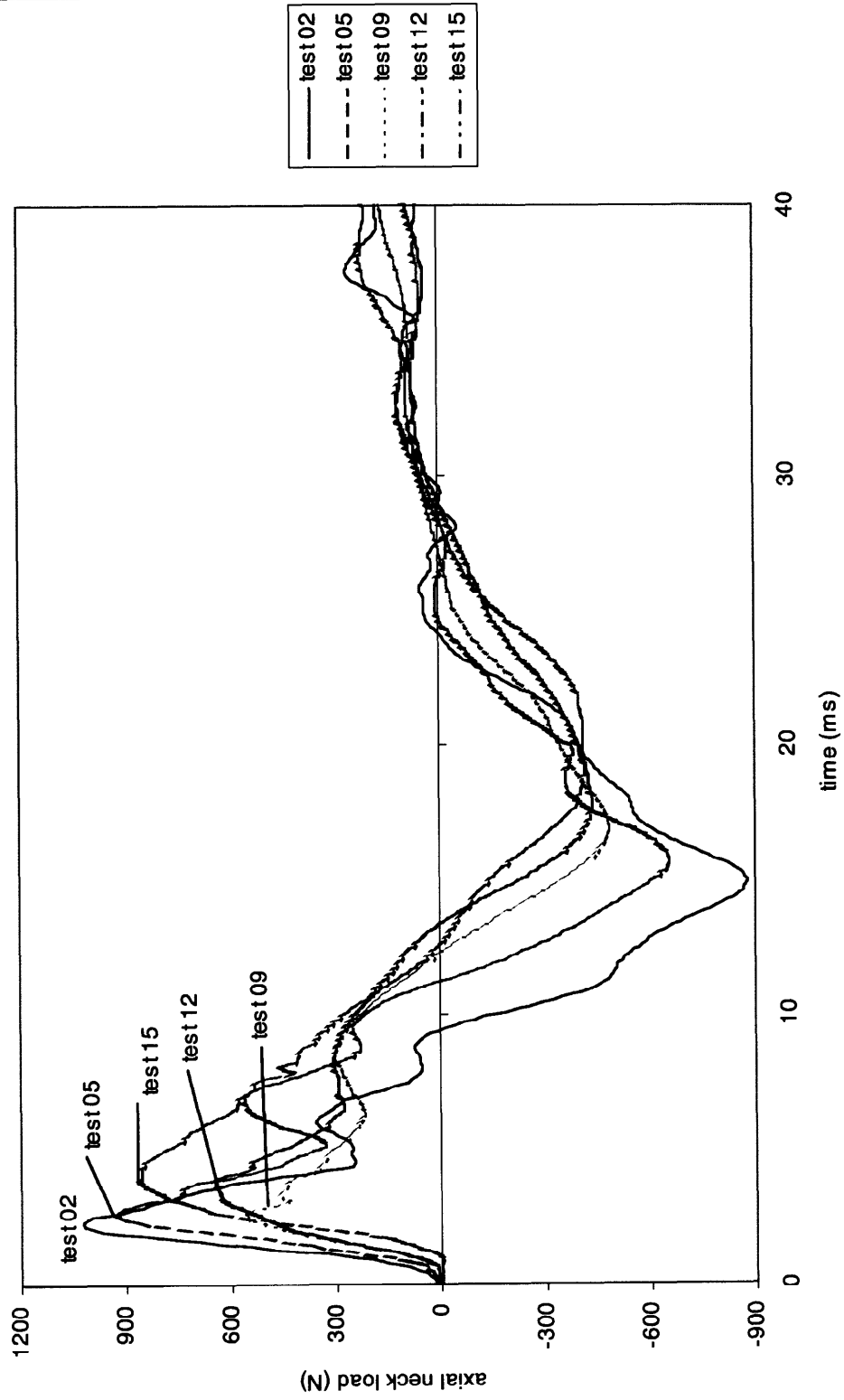


Fig. X.3. X-axis Impacts - Neck Axial Loads (Upper Neck Load Cell)

X-Axis Impacts Moment vs. Angle

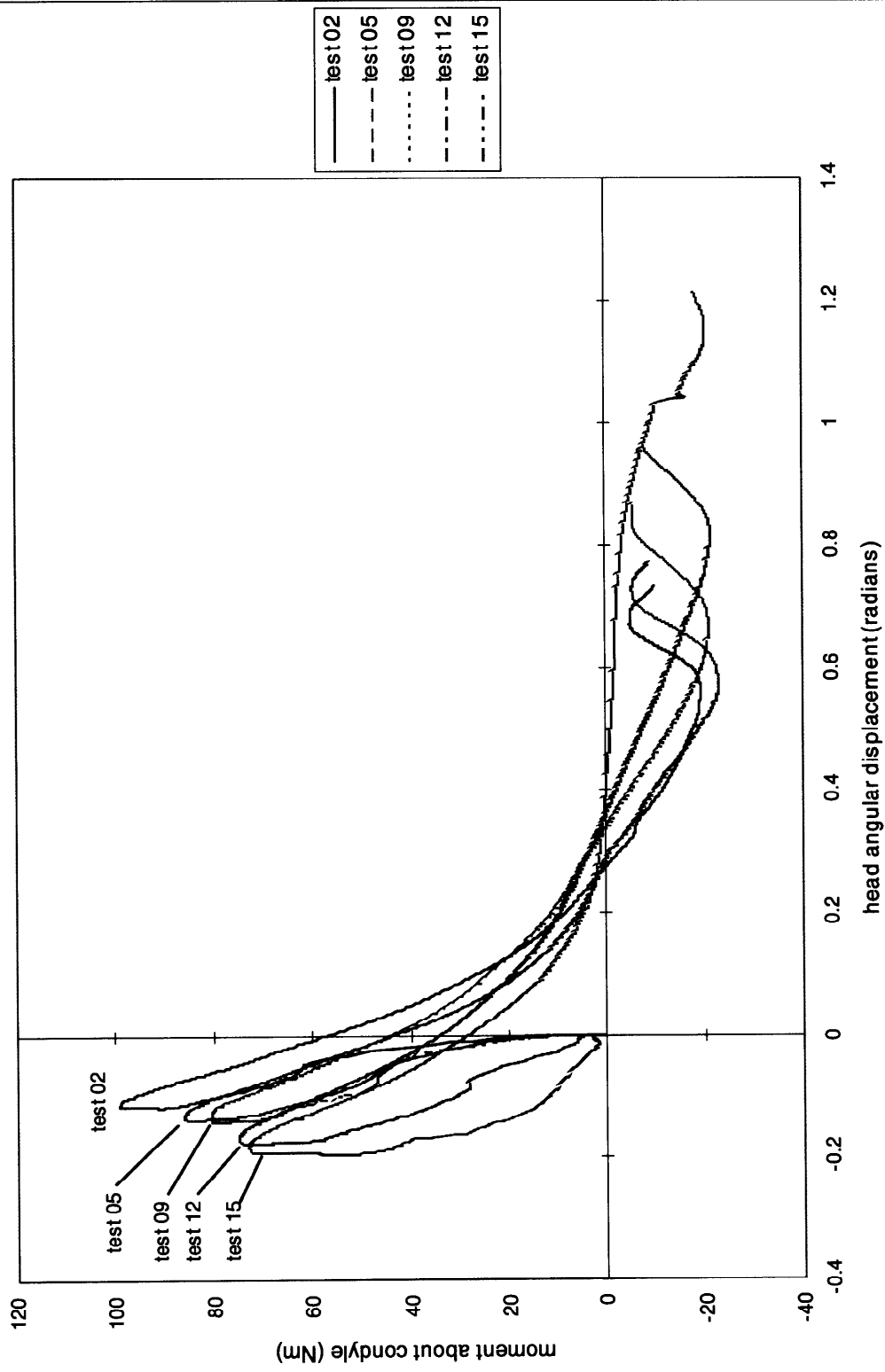


Fig. X.4. X-axis Impacts - Moment versus Head Rotation Angle

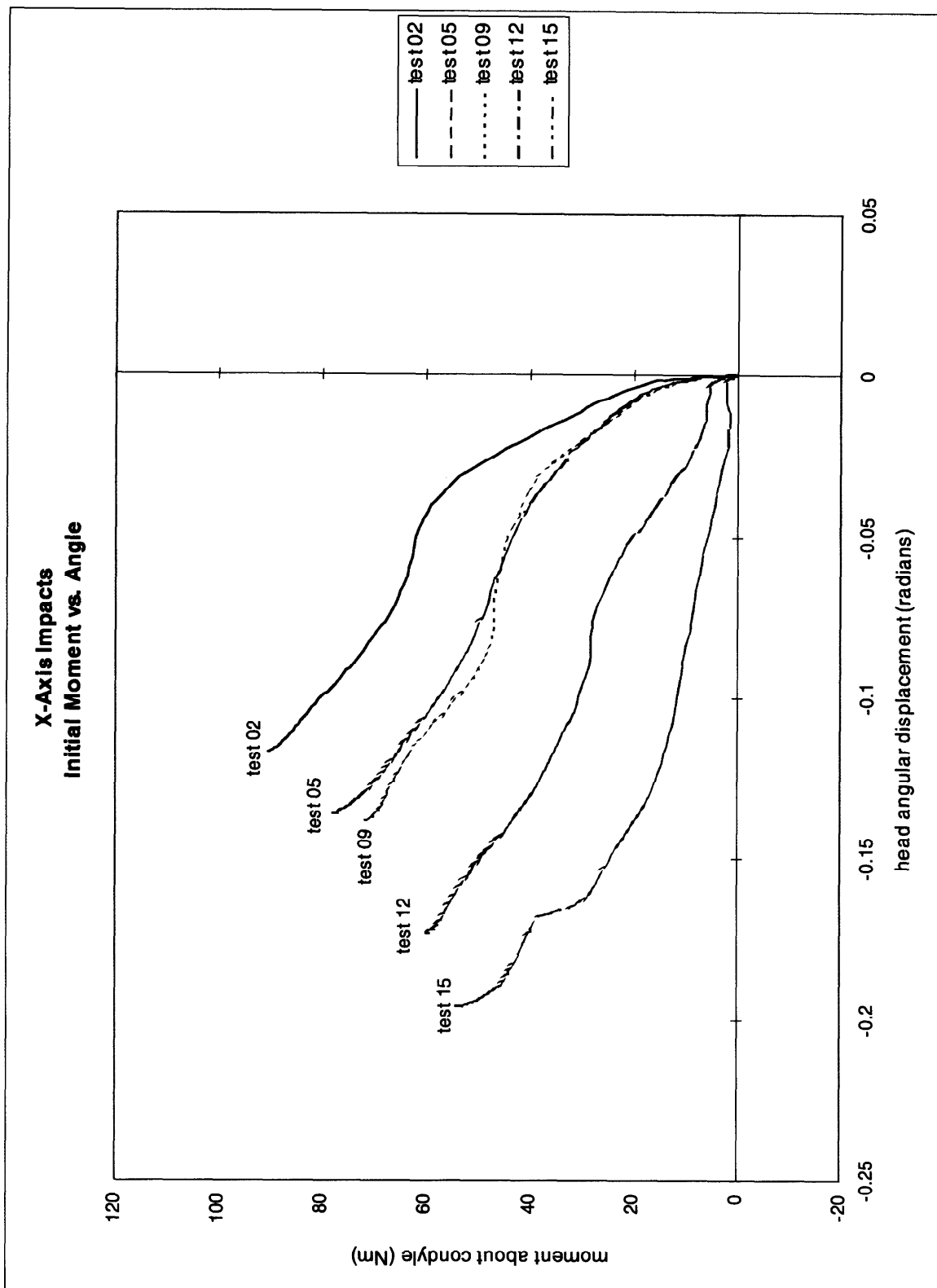


Fig. X.5. X-axis Impacts - Initial Moment Onset versus Head Rotation Angle

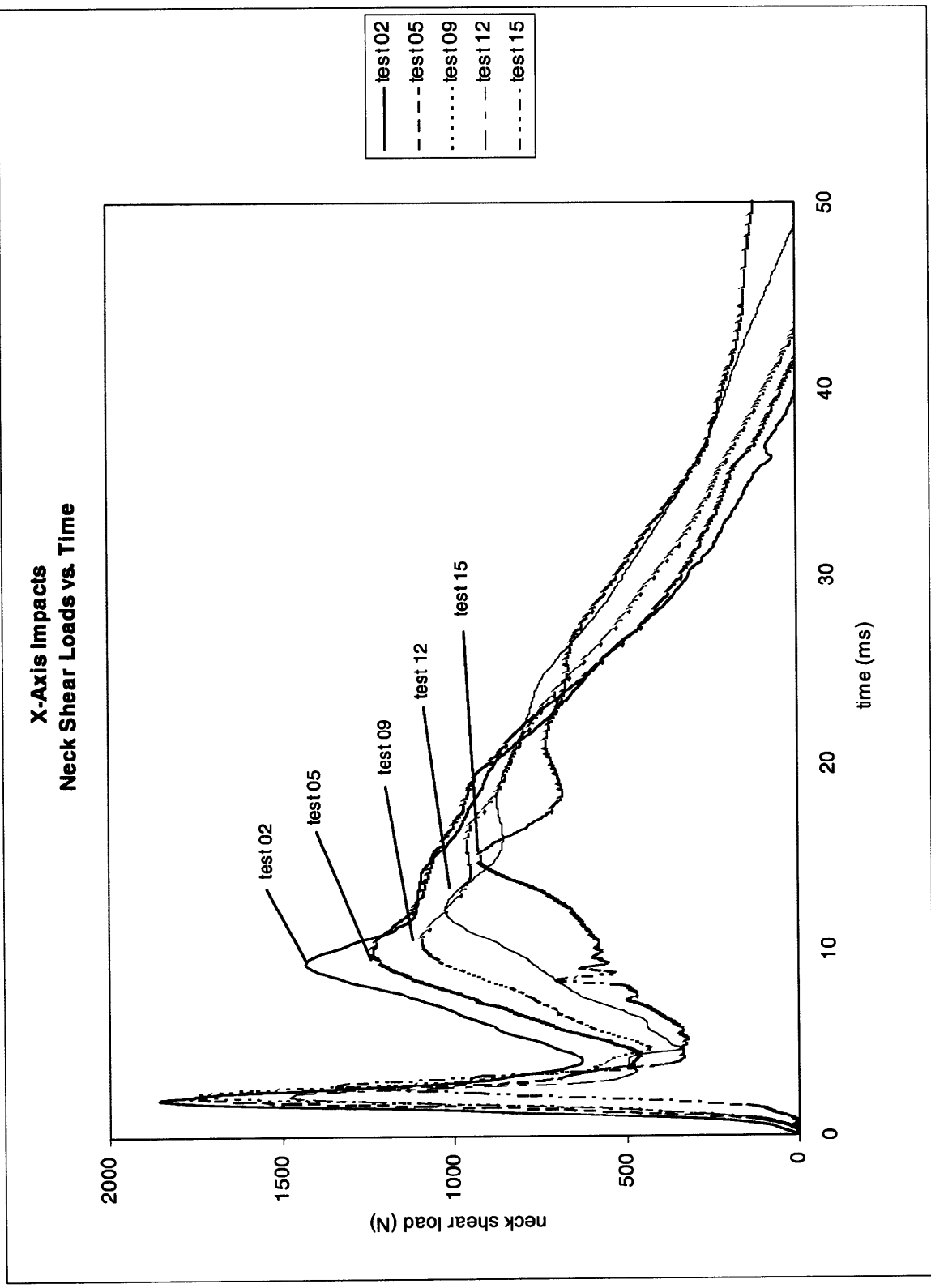


Fig. X.6. X-axis Impacts - Neck Shear Loading (Upper Neck Load Cell)

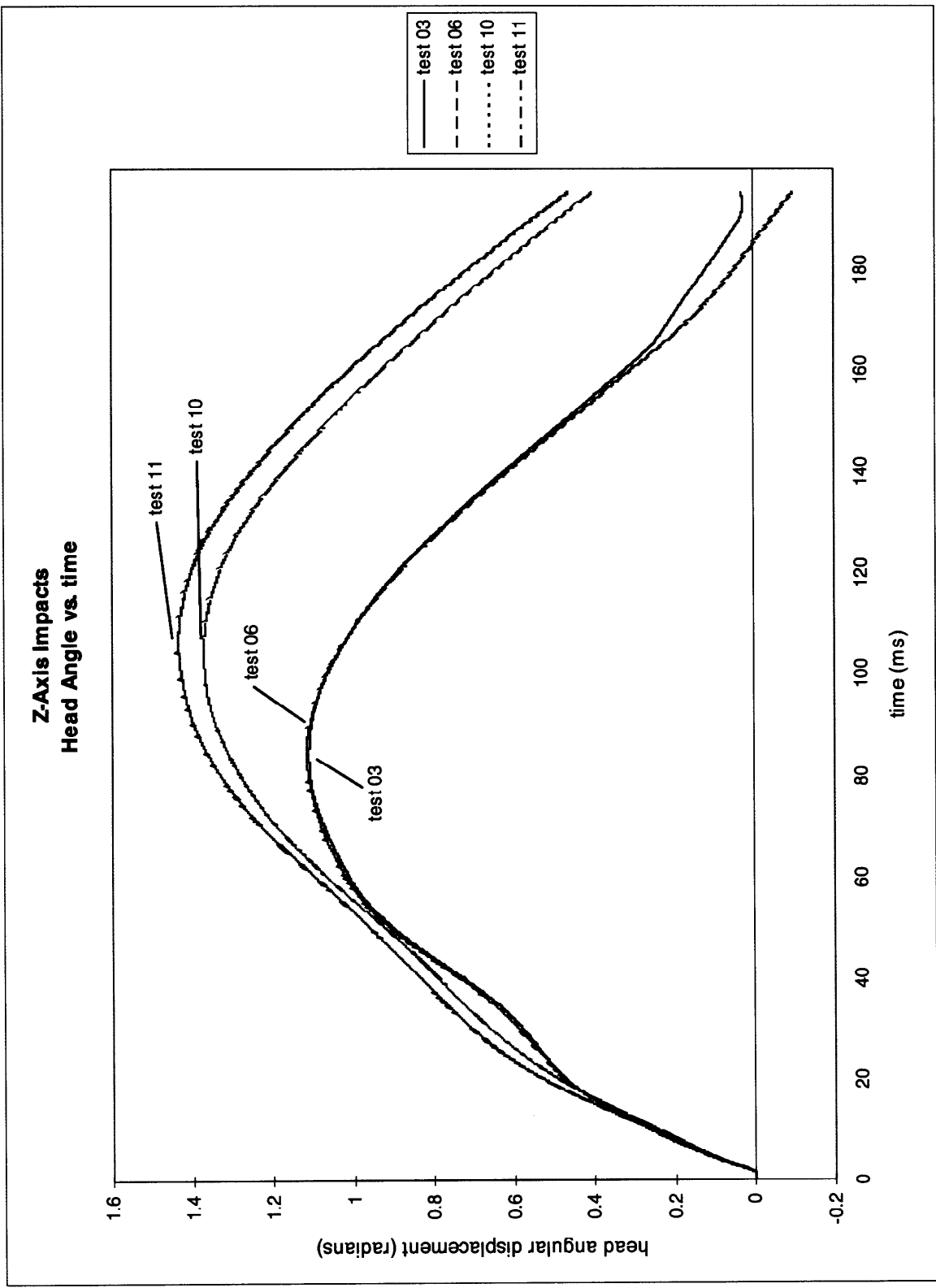


Fig. Z.1. Z-axis Impacts - Head Angular Rotation

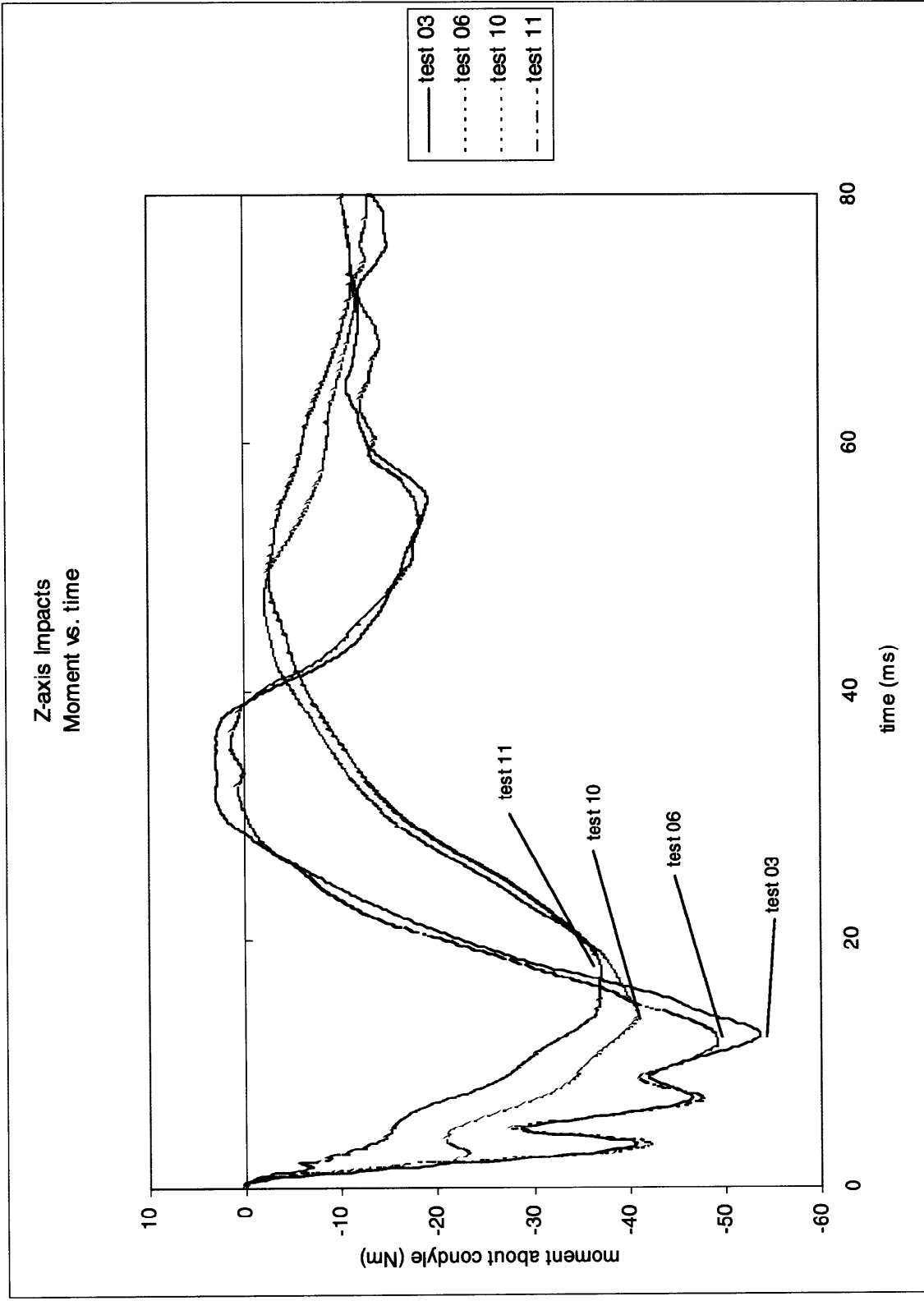


Fig. Z.2. Z-axis Impacts - Neck Moment About Occipital Condyle

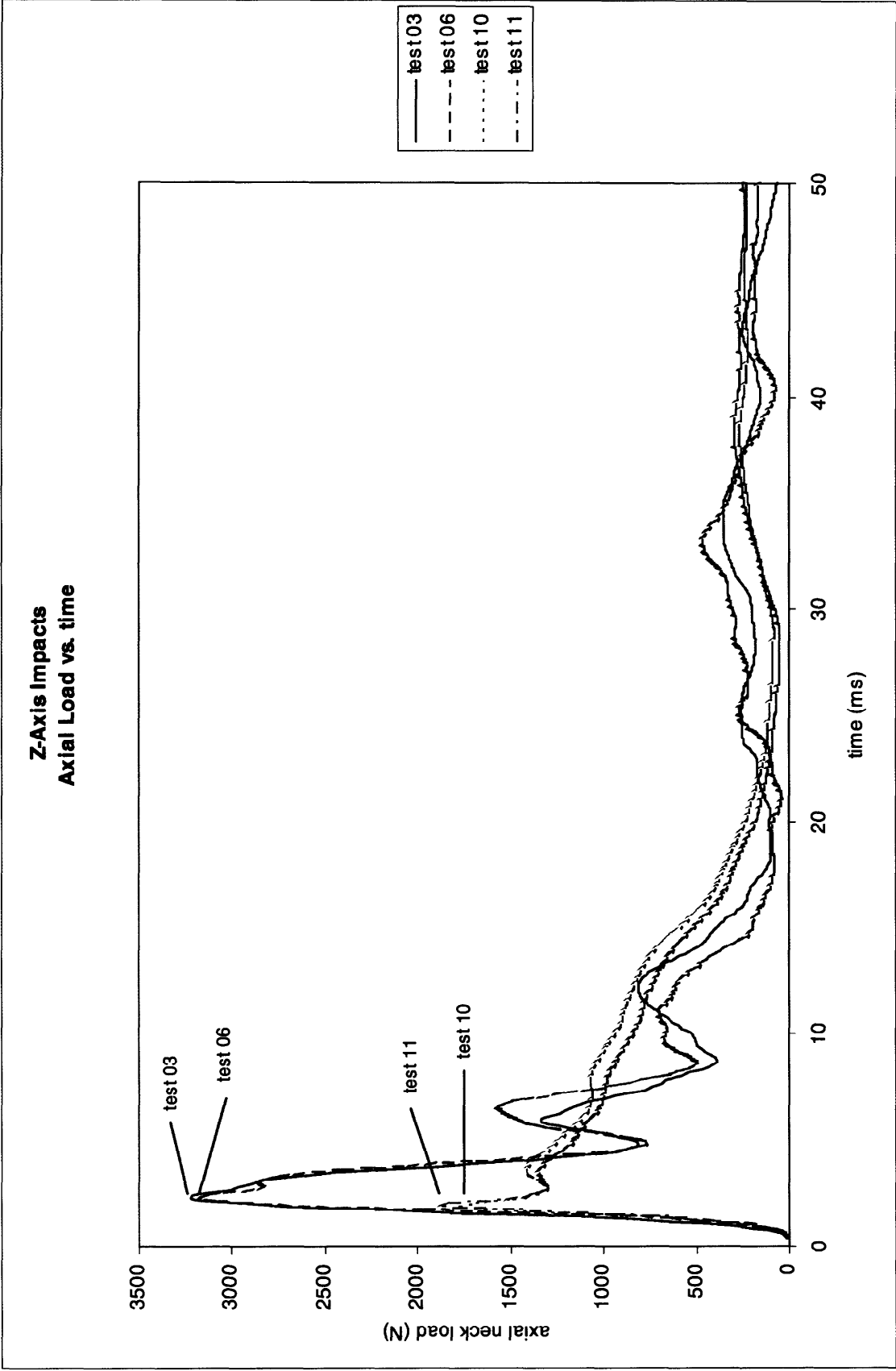


Fig. Z.3. Z-axis Impacts - Neck Axial Loads (Upper Neck Load Cell)

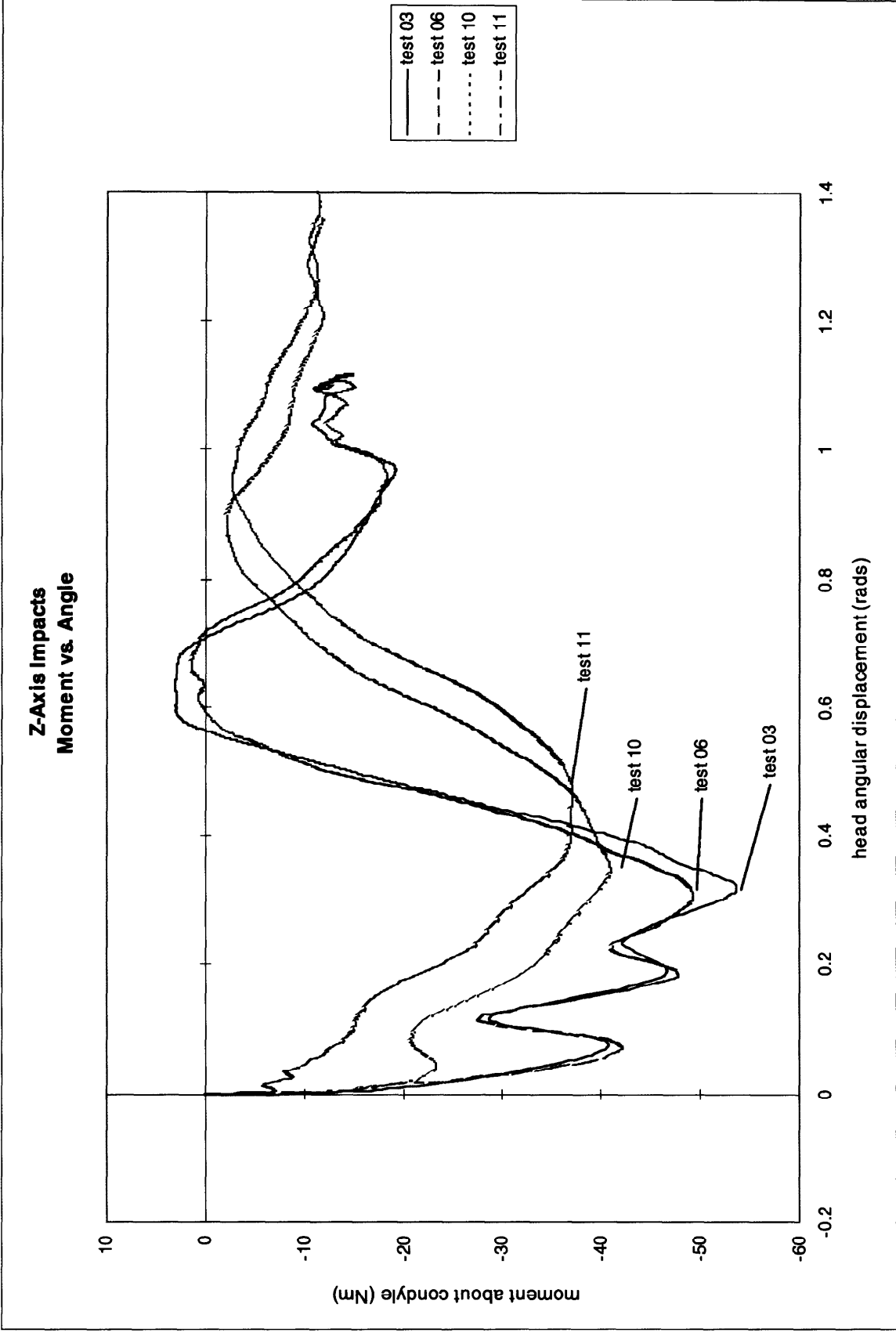


Fig. Z.4. Z-axis Impacts - Neck Moment versus Head Rotation Angle

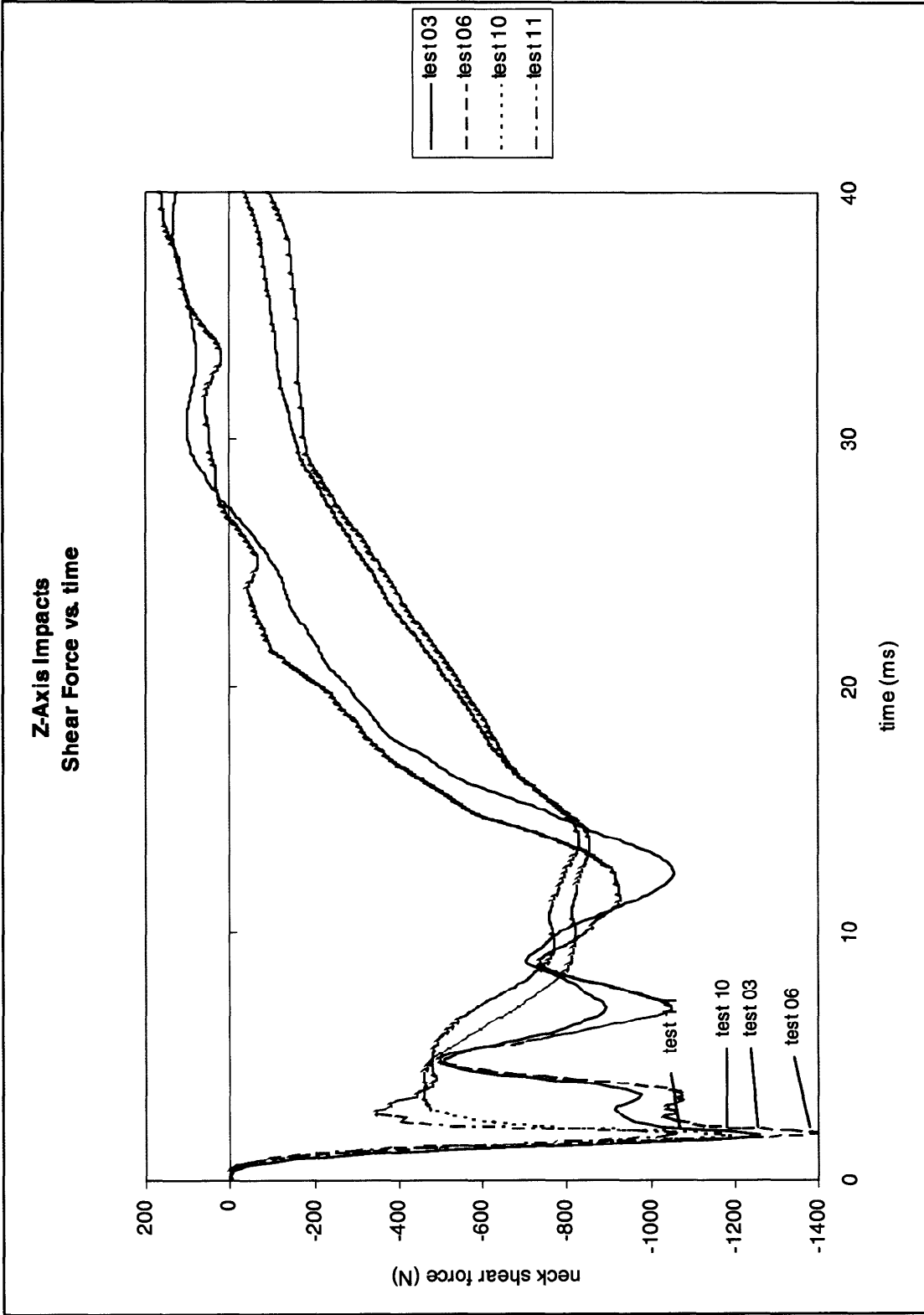


Fig. Z.5. Z-axis Impacts - Neck Shear Loading (Upper Neck Load Cell)